

Thermal Stability of Nickel Cobalt Manganese/Lithium Titanate Battery System Postprint

Authors: Wu Ke, Feng Lihua, Chen Man, Liu Bangjin, flat, Wang Qingsong

Date: 2023-03-18T00:00:00+00:00

Abstract

The thermal stability of primary materials in lithium titanate batteries was examined using a C80 microcalorimeter, analyzing the thermal decomposition of cathode and anode materials, their reaction thermal characteristics with the electrolyte, and the reaction thermal characteristics of the battery system. The results demonstrate that when Ni-Co-Mn ternary cathode material coexists with electrolyte, it undergoes two exothermic processes under heating conditions, with a total reaction heat of $-526.0 \text{ J} \cdot \text{g}^{-1}$ and a reaction activation energy of $273.8 \text{ kJ} \cdot \text{mol}^{-1}$; when $\text{Li}_4\text{Ti}_5\text{O}_{12}$ anode material coexists with electrolyte, it experiences four exothermic processes under heating conditions, with a total reaction heat of $-291.5 \text{ J} \cdot \text{g}^{-1}$ and a reaction activation energy of $61.8 \text{ kJ} \cdot \text{mol}^{-1}$. The exothermic reaction profile of the lithium titanate full-cell system represents a superposition of the reaction processes from the cathode and anode coexisting with the electrolyte; the initiation of thermal runaway is primarily caused by the thermal reaction between the anode and electrolyte, whereas the principal heat contribution during thermal runaway originates from the exothermic reaction between the cathode and electrolyte.

Full Text

Preamble

Vol. 29 No. 1

CHINESE JOURNAL OF MATERIALS RESEARCH

January 2015

Thermal Stability of $\text{Li}(\text{Ni}_x\text{Co}_y\text{Mn}_z)\text{O}_2/\text{Li}_4\text{Ti}_5\text{O}_{12}$ Battery System

Wu Ke¹, Feng Lihua², Chen Man¹, Liu Bangjin¹, Ping Ping², Wang Qingsong²

¹ China Southern Power Grid Power Generation Company, Guangzhou 511400, China

² State Key Laboratory of Fire Science, University of Science and Technology of China, Hefei 230026, China

Supported by National Natural Science Foundation of China (No. 51176183) and National High Technology Research and Development Program of China (No. 2011AA05A111).

Manuscript received June 13, 2014; in revised form July 2, 2014.

Abstract

The thermal stability of the main constructive materials for Li(NixCoyMnz)O₂/Li₄Ti₅O₁₂ batteries was evaluated using a C80 micro calorimeter. The thermal decomposition of the anode and cathode, the heat of reactions between electrolyte and electrodes, and the heat of reactions of an integral cell were characterized. The results show that with rising temperature, the Li(NixCoyMnz)O₂ cathode/electrolyte system undergoes two exothermic processes with a total heat generation of $-526.0 \text{ J} \cdot \text{g}^{-1}$ and activation energy of $273.8 \text{ kJ} \cdot \text{mol}^{-1}$. Meanwhile, the Li₄Ti₅O₁₂ anode/electrolyte system undergoes four exothermic processes with a total heat generation of $-291.5 \text{ J} \cdot \text{g}^{-1}$ and activation energy of $61.8 \text{ kJ} \cdot \text{mol}^{-1}$. The reaction processes for an integral cell represent the overlap of the reaction processes occurring in the two half-cell systems. The thermal runaway phenomenon is triggered by reactions of the anode/electrolyte, while the main heat source may come from reactions of the cathode/electrolyte.

KEY WORDS inorganic non-metallic materials, lithium ion battery, Li₄Ti₅O₁₂, thermal stability

Introduction

Lithium-ion batteries are widely used in various electronic products, electric vehicles, and energy storage systems due to their high energy density, high output power, long charge-discharge cycle life, environmental friendliness, wide operating temperature range, low self-discharge, high voltage, and stable discharge characteristics. However, lithium-ion batteries can explode when heat accumulates during overcharging, and they are also prone to explosion during accidental short circuits or thermal radiation. The explosion of lithium-ion batteries is primarily caused by exothermic chemical reactions between battery materials. Possible exothermic reactions include electrolyte reactions at the anode, thermal decomposition of electrolyte, and electrolyte oxidation at the cathode. The heat released from these reactions increases battery temperature, which in turn accelerates the reactions. When heat accumulation reaches a certain level, explosion may occur.

Currently, research on the thermal stability of lithium-ion battery materials mainly uses Accelerating Rate Calorimeters (ARC) or Differential Scanning Calorimeters (DSC). However, due to inherent limitations, ARC can only detect exothermic reactions and cannot measure reactions with endothermic phe-

nomena, resulting in some discrepancy between experimental results and actual processes. When using DSC, gases produced during reactions cause a significant increase in internal pressure, leading to overflow of reaction products and altered experimental conditions that fail to reflect the true chemical reaction process. The C80 micro calorimeter is a new generation of highly sensitive thermal analyzer that effectively addresses these issues. This study employs a C80 micro calorimeter to investigate the exothermic characteristics of nickel-cobalt-manganese ternary cathode material ($\text{Li}(\text{Ni}_x\text{Co}_y\text{Mn}_z)\text{O}_2$, NCM), lithium titanate anode material ($\text{Li}_4\text{Ti}_5\text{O}_{12}$), electrode materials with electrolyte, and full batteries to analyze the main heat generation processes inside lithium-ion batteries.

1. Experimental

1.1 Sample Preparation

The nickel-cobalt-manganese ternary $\text{Li}(\text{Ni}_x\text{Co}_y\text{Mn}_z)\text{O}_2$ cathode material, lithium titanate $\text{Li}_4\text{Ti}_5\text{O}_{12}$ anode material, and 1 mol/L LiPF_6 /ethylene carbonate (EC)+diethyl carbonate (DEC)+dimethyl carbonate (DMC) electrolyte were all commercial products. The $\text{Li}(\text{Ni}_x\text{Co}_y\text{Mn}_z)\text{O}_2$ electrode consisted of 90% $\text{Li}(\text{Ni}_x\text{Co}_y\text{Mn}_z)\text{O}_2$, 5% acetylene black, and 5% polyvinylidene fluoride (PVDF). The $\text{Li}_4\text{Ti}_5\text{O}_{12}$ electrode consisted of 84% $\text{Li}_4\text{Ti}_5\text{O}_{12}$, 8% acetylene black, and 8% PVDF. After slurry preparation, electrodes were coated onto aluminum foil using a 400 μm blade to form current collectors. The collectors were dried overnight in an oven at 110°C , then punched into 14 mm diameter circular electrodes using a cutting machine.

The electrodes were placed in an argon glove box to assemble CR2032 coin half-cells. The cells used $\text{Li}(\text{Ni}_x\text{Co}_y\text{Mn}_z)\text{O}_2$ or $\text{Li}_4\text{Ti}_5\text{O}_{12}$ electrodes as the cathode, lithium foil as the anode, and polypropylene/polyethylene bilayer membrane (PP/PE) as the separator. The $\text{Li}(\text{Ni}_x\text{Co}_y\text{Mn}_z)\text{O}_2$ cathode half-cells were charged at 0.1 C rate to 4.2 V, then discharged to 2.0 V for 1.5 cycles, and finally charged to 4.2 V with constant voltage charging for 1 hour. The $\text{Li}_4\text{Ti}_5\text{O}_{12}$ anode half-cells were discharged at 0.1 C rate to 1.0 V.

The charged cathode half-cells (4.2 V state) and discharged anode half-cells (1.0 V state) were disassembled in the argon glove box to obtain electrode sheets, which were washed twice with DMC to remove residual LiPF_6 from the active materials. The washed electrode sheets were dried in the glove box for 2 hours to evaporate DMC, after which the active materials were gently scraped off with a spatula. The active materials and electrolyte were added to a high-pressure reaction cell for C80 experiments. The mass ratio of cathode active material to electrolyte was 2.48:1, and the anode active material to electrolyte ratio was 2.45:1. Heat generation per unit mass was calculated based on the total mass of active material and electrolyte.

1.2 Experimental Apparatus

The C80 micro calorimeter is suitable for measuring thermal characteristics of chemical reactions. Its temperature range is from ambient to 300°C, with constant temperature control accuracy of $\pm 0.001^\circ\text{C}$, heating rate range of $0.01\text{--}2.00^\circ\text{C}\cdot\text{min}^{-1}$, resolution of 0.1mW , sensitivity limit of $1\mu\text{W}$, and sample mass of $1\text{--}10\text{g}$. The experiments used identical reference and reaction cells.

2. Results and Discussion

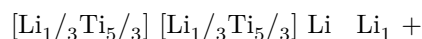
2.1 Thermal Stability of Cathode $\text{Li}(\text{Ni}_x\text{Co}_y\text{Mn}_z)\text{O}_2$ and its Coexistence with Electrolyte

[Figure 1: see original paper] shows the heat flow curve of delithiated $\text{Li}(\text{Ni}_x\text{Co}_y\text{Mn}_z)\text{O}_2$ cathode material during heating. The material exhibits virtually no exothermic reaction before 170.4°C . Between 170.4°C and 213.5°C , an exothermic peak appears, reaching its maximum at 194.7°C with a heat release of $-7.8\text{ J}\cdot\text{g}^{-1}$, likely corresponding to decomposition of metastable surface species on the cathode. Subsequently, $\text{Li}(\text{Ni}_x\text{Co}_y\text{Mn}_z)\text{O}_2$ continues to release heat until the test ends at 300°C , with a total heat release of $-52.2\text{ J}\cdot\text{g}^{-1}$. These results demonstrate that nickel-cobalt-manganese ternary cathode material possesses good thermal stability, consistent with other studies showing stable cycling performance and high reversible capacity at elevated temperatures.

[Figure 2: see original paper] presents the heat flow curve for the coexistence system of $\text{Li}(\text{Ni}_x\text{Co}_y\text{Mn}_z)\text{O}_2$ and electrolyte. With increasing temperature, this system undergoes a minor exothermic process beginning at 193.0°C , peaking at 232.7°C with a heat release of $-44.6\text{ J}\cdot\text{g}^{-1}$. A vigorous exothermic reaction then initiates at 270.1°C , reaching a peak at 289.5°C with a heat release of $-481.4\text{ J}\cdot\text{g}^{-1}$. The total heat release for the entire process is $-526.0\text{ J}\cdot\text{g}^{-1}$. When the first small exothermic peak in [Figure 2: see original paper] is magnified and compared with the heat flow curve of pure $\text{Li}(\text{Ni}_x\text{Co}_y\text{Mn}_z)\text{O}_2$ from [Figure 1: see original paper], the results indicate that this stage represents heat release from $\text{Li}(\text{Ni}_x\text{Co}_y\text{Mn}_z)\text{O}_2$ alone, while the subsequent sharp exothermic peak corresponds to the violent exothermic reaction between $\text{Li}(\text{Ni}_x\text{Co}_y\text{Mn}_z)\text{O}_2$ and electrolyte. Due to the rapid release of substantial heat, explosion may occur if this heat is not dissipated promptly.

2.2 Thermal Stability of Anode $\text{Li}_4\text{Ti}_5\text{O}_{12}$ and its Coexistence with Electrolyte

Spinel-structured $\text{Li}_4\text{Ti}_5\text{O}_{12}$ exhibits excellent cycling performance and a high, stable operating voltage, making it a promising anode material for lithium-ion batteries. The charge-discharge reaction of $\text{Li}_4\text{Ti}_5\text{O}_{12}$ proceeds as follows:



Thermal analysis of lithiated Li₄Ti₅O₁₂ using C80 yields the heating heat flow curve shown in [Figure 3: see original paper]. The lithiated Li₄Ti₅O₁₂ begins to release heat at 185.9°C, reaching a peak at 223.5°C with total heat release of $-71.5 \text{ J} \cdot \text{g}^{-1}$. Above 282.8°C, a small endothermic peak appears at 293.5°C with heat absorption of $0.4 \text{ J} \cdot \text{g}^{-1}$.

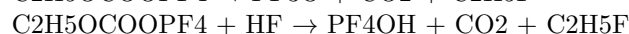
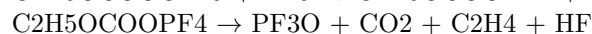
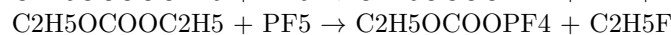
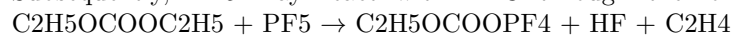
[Figure 4: see original paper] shows the heating heat flow curve for the Li₄Ti₅O₁₂/electrolyte coexistence system, which exhibits four exothermic stages. The first sharp exothermic peak occurs between 89.2–107.1°C, peaking at 94.7°C with heat release of $-32.9 \text{ J} \cdot \text{g}^{-1}$. Although the heat generation is small, occurring in the low-temperature region, it may trigger additional reactions through heat accumulation. The second exothermic stage spans 107.1–172.5°C, peaking at 141.5°C with heat release of $-71.1 \text{ J} \cdot \text{g}^{-1}$. The third stage ranges from 172.5–233.1°C, peaking at 209.2°C with heat release of $-97.8 \text{ J} \cdot \text{g}^{-1}$. The final exothermic stage is relatively 平缓, peaking at 264.2°C with heat release of $-89.7 \text{ J} \cdot \text{g}^{-1}$. The total heat release for these four stages is $-291.5 \text{ J} \cdot \text{g}^{-1}$.

The electrolyte in [Figure 4: see original paper] contains EC, DEC, and DMC, making the reaction process complex. To analyze each exothermic peak in [Figure 4: see original paper], thermal analysis was performed on 1.0 mol/L LiPF₆/EC+DEC and 1.0 mol/L LiPF₆/EC+DMC, with heat flow curves shown in [Figure 5: see original paper]. Their exothermic peak temperatures are 194°C and 204°C, respectively. In [Figure 4: see original paper], the third exothermic peak of the Li₄Ti₅O₁₂/electrolyte system occurs at 209.2°C, which is close to these temperatures. Therefore, this stage involves not only thermal decomposition of Li₄Ti₅O₁₂ itself but also electrolyte decomposition.

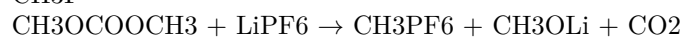
LiPF₆ in electrolyte readily undergoes the reaction: $\text{LiPF}_6(\text{s}) \rightarrow \text{LiF}(\text{s}) + \text{PF}_5$

PF₅ is a strong Lewis acid that disrupts the cyclic structure of EC, causing an endothermic reaction that decomposes into polyethylene oxide (PEO) polymer and carbon dioxide. As shown in [Figure 5: see original paper], the endothermic peak at 180°C corresponds to this reaction.

Subsequently, PF₅ may react with DEC through the following reactions:



PF₅ may also react with DMC: $\text{CH}_3\text{OCOCH}_3 + \text{PF}_5 \rightarrow \text{CH}_3\text{OCOOPF}_4 + \text{CH}_3\text{F}$



Compared with the thermal behavior of Li₄Ti₅O₁₂ without electrolyte, adding electrolyte reduces the reaction onset temperature to 89.2°C. As temperature increases, the coexistence system generates heat more rapidly, showing distinct

exothermic peaks at 94.7°C, 141.5°C, 209.2°C, and 264.2°C, producing significantly more heat. If heat generated in the low-temperature stage is not dissipated promptly, battery temperature will rise, potentially causing thermal runaway.

2.3 Thermal Effects of Full Li₄Ti₅O₁₂ Cell

[Figure 6: see original paper] shows the relationship between heat flow curves and temperature for the full cell, cathode/electrolyte, anode/electrolyte, and separator. For clarity, overlapping curves are magnified. Since unit mass heat flow is calculated as the ratio of measured heat flow to total system mass, and the full cell mass is larger than other systems, the full cell's heat flow peaks appear smaller than those of the corresponding cathode/electrolyte or anode/electrolyte mixtures. The full cell reaction stages are:

- 1) The earliest exothermic reaction in the full cell system involves metastable substances on the lithium titanate anode surface. The anode/electrolyte system begins releasing heat at 89.2°C, reaching its first exothermic peak at 94.7°C. In the full cell thermal behavior, a small exothermic peak appears between 85–100°C, peaking at 89.6°C with heat release of $-4.9 \text{ J} \cdot \text{g}^{-1}$. The close agreement between these peaks confirms this process as decomposition of metastable substances on the anode surface. Although the heat release is small, it provides initial heat accumulation for subsequent reactions, leading to temperature increase.
- 2) As temperature increases, the full cell system begins slowly releasing heat again at 123.5°C. Since the cathode material shows no significant exothermic reaction in this temperature range, this gradual heat release is primarily caused by anode/electrolyte reactions between 125–200°C.
- 3) At 171.5°C, the full cell system shows a small endothermic dip that reduces heat release between 125–200°C, with heat generation resuming only above 175°C. Analysis of separator thermal behavior indicates this process mainly results from separator melting and heat absorption.
- 4) Between 175–213.5°C, the full cell system exhibits exothermic behavior, slightly more intense than in stage 2. This enhancement occurs because as the separator melts, cathode and anode materials gradually contact each other, causing internal short circuits that trigger additional short-circuit heat generation.
- 5) A large exothermic peak appears from 213.5°C to 256.2°C, peaking at 230.9°C. Comparative analysis with cathode/electrolyte and anode/electrolyte systems reveals this peak results from combined thermal reactions of anode material with electrolyte (200–227°C) and cathode material with electrolyte (200–260°C). As the analysis shows, heat generation in this stage primarily comes from the cathode/electrolyte system, making the cathode reaction between 200–260°C dominant. The

total reaction heat for this process is $-558.7 \text{ J} \cdot \text{g}^{-1}$.

- 6) Above 250°C , heat release from the full cell becomes insignificant, indicating the main reactions have concluded.

These analyses demonstrate that heat accumulation inside the battery is initially triggered by decomposition of metastable substances on the lithium titanate anode surface. Subsequently, both cathode and anode react with electrolyte, but the cathode/electrolyte reaction releases the most heat. The high-temperature reaction between cathode material and electrolyte is the primary cause of violent combustion or even explosion.

2.4 Thermal Decomposition Kinetics of Electrode Materials

Based on heat flow data from electrode materials and full cells during heating, thermodynamic and kinetic parameters of exothermic decomposition reactions can be calculated, including reaction heat, reaction order, activation energy, and pre-exponential factor. Assuming electrode material thermal decomposition and reactions with electrolyte follow Arrhenius kinetics with first-order reactions, the reaction rate equation based on heating heat flow data is:

$$dx/dt = A \cdot \exp(-E/RT) \cdot (1-x)^n$$

where $x = (M_0 - M)/M_0$ is the conversion percentage, A is the pre-exponential factor (s^{-1}), E is the activation energy ($\text{J} \cdot \text{mol}^{-1}$), R is the gas constant ($\text{J} \cdot \text{K}^{-1} \cdot \text{mol}^{-1}$), T is the system temperature (K), n is the reaction order, and t is time (s). M is the reactant mass at any time (g), and M_0 is the initial reactant mass (g).

Substituting x into the equation yields: $dM/dt = -A \cdot \exp(-E/RT) \cdot M$

The heat release per unit mass is ΔH : $\Delta H = (1/M_0) \int_{t_0}^t q \, dt$

where t_0 is the reaction start time and t is the reaction end time.

Substituting equation (3) into equation (2) gives the chemical reaction heat release equation: $q = \Delta H \cdot A \cdot \exp(-E/RT)$

Taking the natural logarithm of equation (4): $\ln(q) = \ln(\Delta H \cdot A) - E/(RT)$

By plotting $\ln(q)$ versus $1/T$ and selecting the initial reaction stage for linear regression, a straight line is obtained. The slope and intercept yield the pre-exponential factor A and activation energy E . Activation energy characterizes the energy required for reactants to reach the activated state; higher values indicate more difficult reactions. The pre-exponential factor represents the probability of reaction per collision.

[Figure 7: see original paper] shows the $\ln(q)$ versus $1/T$ curve for the $\text{Li}_4\text{T}_i\text{O}_{12}$ /electrolyte coexistence system. From the slope, the activation energy is calculated as $61.8 \text{ kJ} \cdot \text{mol}^{-1}$ and the pre-exponential factor as

$9.8 \times 10^2 \text{ s}^{-1}$. Using the same method, other systems' parameters were obtained, as listed in .

Comparison of the thermodynamic and kinetic parameters reveals that the anode/electrolyte coexistence system has the lowest activation energy ($61.8 \text{ kJ} \cdot \text{mol}^{-1}$), indicating it is most prone to chemical reaction and thus has the poorest thermal stability. The cathode/electrolyte system has higher activation energy ($273.8 \text{ kJ} \cdot \text{mol}^{-1}$), demonstrating better thermal stability than the anode/electrolyte system. However, without electrolyte, the cathode material has lower activation energy than the anode material, and its thermal decomposition begins 15.5°C lower, indicating that NCM cathode material alone is less thermally stable than $\text{Li}_4\text{Ti}_5\text{O}_{12}$ anode material.

Conclusions

1. Single NCM cathode material or lithium titanate anode material releases little heat and exhibits high thermal stability during heating. When coexisting with electrolyte, heat generation increases and thermal stability decreases. For NCM cathode mixed with electrolyte, the first reaction heat increases from $-7.8 \text{ J} \cdot \text{g}^{-1}$ to $-44.6 \text{ J} \cdot \text{g}^{-1}$, and the total reaction heat increases to $-526.0 \text{ J} \cdot \text{g}^{-1}$. For lithium titanate anode mixed with electrolyte, the reaction onset temperature decreases from 185.9°C to 89.2°C , and total heat release increases from $-71.5 \text{ J} \cdot \text{g}^{-1}$ to $-291.5 \text{ J} \cdot \text{g}^{-1}$.
2. The exothermic reaction processes experienced by the full cell system represent the superposition of heat generation from cathode/electrolyte and anode/electrolyte systems, with total reaction heat of $-558.7 \text{ J} \cdot \text{g}^{-1}$. In the later stage of cathode/electrolyte reaction, insufficient heat dissipation may lead to explosion.
3. The anode/electrolyte coexistence system has the smallest activation energy and is most susceptible to chemical reaction. The cathode/electrolyte system has higher activation energy and better thermal stability than the anode/electrolyte system. However, the cathode/electrolyte system generates substantial heat at high temperatures, and once triggered, the consequences can be more severe, potentially causing explosion.

References

1. Wang Qingsong, Sun Jinhua, Yao Xiaolin, Chen Chunhua. Thermal behavior inside lithium-ion batteries. *Chinese Journal of Applied Chemistry*, 23(5), 489 (2006).
2. Wang Qingsong, Sun Jinhua, Chen Sining, Yao Xiaolin, Chen Chunhua. Research progress in thermal safety of Li-ion batteries. *Battery Bimonthly*, 135(3), 240 (2005).

3. Thermal runaway caused fire and explosion of lithium ion battery. *Journal of Power Sources*, 208, 210 (2012).
4. Sun Jinhua, Li Xinran, Hasegawa K, Liao Guoxing. Thermal hazard evaluation of complex reactive substance using calorimeters and dewar vessel. *Journal of Thermal Analysis and Calorimetry*, 6(3), 883 (2004).
5. Wang Qingsong, Sun Jinhua. Study on the materials thermal properties of lithium ion secondary batteries by using C80 calorimeter. *Chinese Journal of Power Sources*, 31(8), 592 (2007).
6. Dolotko O, Senyshyn A, Mühlbauer MJ, Nikolowski K, Ehrenberg H. Understanding structural changes in NMC li-ion cells by in situ neutron diffraction. *Journal of Power Sources*, 255, 198 (2014).
7. Wang J, Zhao HL, Wen YT, Xie JY, Xia Q, Zhang TH, Z ZP, Du XF. High performance $\text{Li}_4\text{Ti}_5\text{O}_{12}$ material as anode for lithium-ion batteries. *Electrochimica Acta*, 113, 679 (2013).
8. Scharner S, Weppner W, Schmid-Beurmann P. Evidence of two-phase formation upon lithium insertion into the $\text{Li}_{1.33}\text{Ti}_{1.67}\text{O}_4$. *Journal of the Electrochemical Society*, 146(3), 857 (1999).
9. Kawamura T, Kimura A, Egashira M, Okada S, Yamaki J. Thermal stability of alkyl carbonate mixed-solvent electrolytes for lithium ion cells. *Journal of Power Sources*, 104, 260 (2002).
10. Gnanaraj JS, Zinigrad E, Asraf L, Gottlieb HE, Sprecher M, Schmidt M, Geissler W, Aurbach D. A detailed investigation of the thermal reactions of LiPF_6 solution in organic carbonates using ARC and DSC. *Journal of the Electrochemical Society*, 150, A1533 (2003).
11. Tasaki K, Kanda K, Nakamura S, Ue M. Decomposition of LiPF_6 and stability of PF_5 in li-ion battery electrolytes. *Journal of the Electrochemical Society*, 150, A1628 (2003).
12. Ono Y. Dimethyl carbonate for environmentally benign reactions. *Pure and Applied Chemistry*, 68, 367 (1996).
13. Sun Jinhua, Ding Hui. Evaluation of Chemical Thermal Hazard. Beijing, Science Press, 2005, p. 141-144.

Note: Figure translations are in progress. See original paper for figures.

Source: ChinaXiv – Machine translation. Verify with original.